

RESEARCH ARTICLE

Intra-arterial delivery of endostatin gene to brain tumors prolongs survival and alters tumor vessel ultrastructure

FH Barnett¹, M Scharer-Schuksz¹, M Wood¹, X Yu², TE Wagner² and M Friedlander¹

¹Department of Cell Biology, The Scripps Research Institute, La Jolla, CA, USA; and ²The Oncology Research Institute, Greenville Hospital System, Greenville, SC, USA

Glioblastoma multiforme (GBM) is an incurable malignant brain tumor, usually fatal within 1 year of diagnosis. Using a syngeneic rat 9L gliosarcoma model, we have developed a novel drug delivery method in which naked plasmid DNA is selectively targeted to brain tumors via intra-arterial injection. Using a plasmid encoding the antiangiogenic endostatin, transgene expression can be detected in tumor cells in vivo, and therapeutic efficacy is observed. Administration of this plasmid resulted in an 80% tumor volume reduction 1 week after treatment and enhanced survival time by up to 47%.

Treated tumors exhibited a 40% decrease in the number of tumor vessels; ultrastructural analysis of remaining tumor vessels demonstrated a number of changes including markedly narrowed or collapsed lumens. We conclude that intra-arterial injection of plasmids selectively targets therapeutic genes to CNS neoplasms. This method of gene therapy holds promise for the treatment of these highly malignant brain tumors.

Gene Therapy (2004) 11, 1283–1289. doi:10.1038/sj.gt.3302287; Published online 27 May 2004

Keywords: brain tumors; antiangiogenesis; endostatin

Introduction

Despite surgery, radiation and chemotherapy, patients diagnosed with glioblastoma multiforme (GBM), the most aggressive and common malignant glioma, have a median survival of less than 1 year.¹ Surgical resection alone is unsatisfactory because tumor cells invade and migrate within the surrounding brain tissue. Radiation treatment prolongs survival but is not curative. Chemotherapy has only limited efficacy due to the relative impermeability of the blood–brain barrier (BBB). The blood–tumor barrier (BTB), although more permeable than the normal BBB, allows only limited access of chemotherapeutic agents to the tumor.²

The poor prognosis associated with current therapies and the highly vascular nature of GBM suggest that angiostatic agents may be effective as therapeutics. Advantages of targeting tumor-associated angiogenesis include avoiding drug resistance, since blood vessels are genetically stable³ and selectivity, since active, nontumor-associated angiogenesis in normal adults occurs only during wound healing, ovulation, menstruation and pregnancy.⁴ A number of antiangiogenic molecules have been identified and several are already in clinical trials for the treatment of a variety of malignancies.⁵ Endostatin, a C-terminal proteolytic fragment of collagen XVIII, has been shown to be antiangiogenic and induces

tumor regression in multiple tumor models⁶ via systemic delivery of recombinant protein or through gene therapy.^{7–9} Gene therapy may be preferable to recombinant protein administration since it can provide sustained levels of gene product and, if tumor cells are transduced, a more specific localization of the therapeutic protein to the site of disease.

Effective plasmid delivery to the brain depends on crossing the BTB. Liposome-associated plasmids can pass into brain tumor cells and express transgene with or without BTB disruption, while adenovirus and herpes virus vectors require BTB disruption for significant transgene expression.^{10,11} In this study, we exploit the intrinsic permeability of the BTB to deliver a naked plasmid encoding endostatin. Once expressed, endostatin decreases tumor vascular density, lumen diameter, and permeability without affecting normal brain vessels. This antiangiogenic effect results in reduction of tumor volume and prolonged survival, suggesting that such an approach may be useful for the treatment of currently incurable malignant brain tumors.

Results

The tumor model mirrors the angiogenic and locally invasive behavior of malignant glioma in humans

In order to (1) improve the evaluation of therapeutic efficacy in an animal model and (2) approximate the course of GBM in humans, we studied the time course of tumor vessel development using collagen IV immunohistochemical staining. At 3 days following tumor cell

Correspondence: Dr M Friedlander, Department of Cell Biology, The Scripps Research Institute, 10550 North Torrey Pines Road, MB28, La Jolla, CA 92037, USA

Received 2 September 2003; accepted 25 March 2004; published online 27 May 2004

implantation, tumor cells had not yet formed a solid tumor, and tumor vessels were similar in appearance to those in the surrounding brain tissue (Figure 1a). However, by day 6, vessels were hypertrophic and tortuous, and a collagen IV-containing extracellular matrix had formed (Figure 1b). By day 17, the tumor was less densely packed than at day 6 and the vessels were somewhat less tortuous (Figure 1c). In all, over 650 rats were examined and in no case has there been a failure to form a highly vascularized tumor.

Intra-arterial delivery of naked plasmid specifically targets tumor and satellite tumor foci (STF)

We modified an earlier method for carotid cannulation involving BBB disruption^{10,12} and developed a technique for direct injection into the internal carotid artery without BBB disruption. Intra-arterial injection of pEGFP-N1 plasmid encoding green fluorescent protein (GFP) results in GFP transgene expression by tumor (Figure 2a, outlined area), as well as STF (arrows). Little or no transgene expression is detected in normal brain. We estimated that 10–30% of tumor cells are transduced by this method (detailed in the legend to Figure 3 and discussed further below), somewhat less than what we have previously reported using liposome coats and cytoplasmic expression vectors.¹² Tumor cells, and perhaps endothelial cells associated with the tumor, are the main targets of transduction (Figure 2b, arrows). This result suggests that intra-arterial delivery of naked

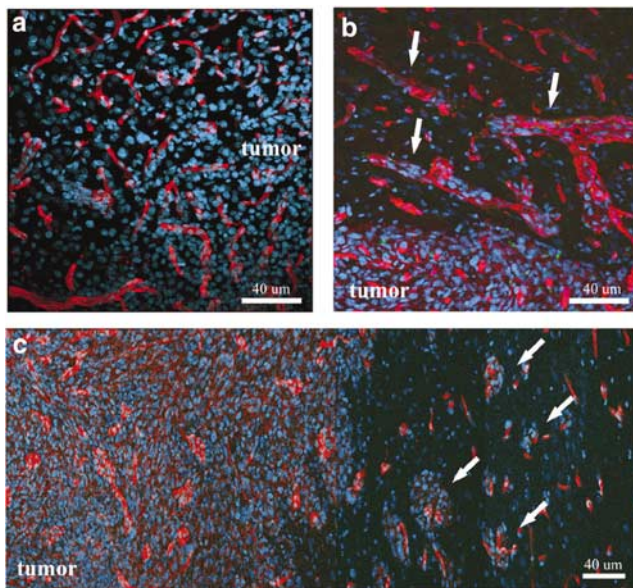


Figure 1 9L tumor model mirrors human GBM. (a) At 3 days following 9L gliosarcoma cell implantation, tumor vasculature still resembled normal blood vessels in appearance (red: collagen IV, blue: DAPI nuclear stain). (b) At 6 days after implantation, vessels were apparent at the tumor periphery (arrows). In addition, increased collagen IV-containing extracellular matrix was present within the tumor parenchyma (red: collagen IV; blue: DAPI nuclear stain). (c) Day 17 9L gliosarcoma-injected brains demonstrated a highly vascularized tumor and nearby STF (arrows). The tumor vessels were less densely packed and markedly hypertrophic compared to surrounding normal, nontumor vessels (Figure 1c). STF were evident and always associated with a vessel (arrows) (red: collagen IV; blue: DAPI nuclear stain). Images: $\times 25$ magnification, scale bars = 40 μm .

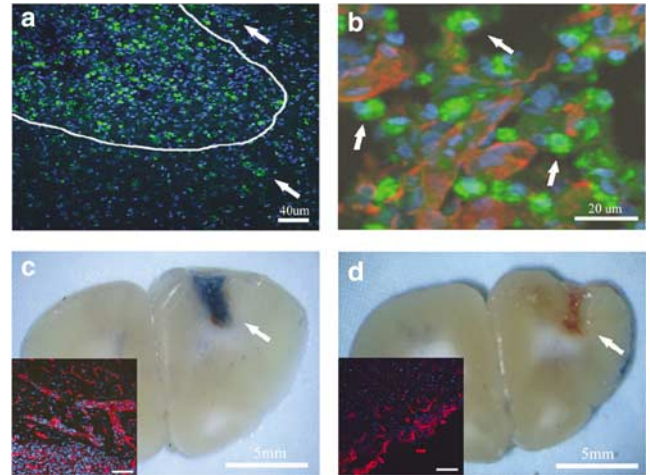


Figure 2 pEGFP-N1 plasmid delivered intra-arterially transduces tumor and STF but not surrounding brain. (a) Intracarotid injection of 40 μg pEGFP-N1 plasmid without BBB disruption leads to expression of the GFP marker gene (green) in tumor (outlined) and STF (arrows), but not in surrounding normal brain (blue: DAPI nuclear stain, scale bar = 40 μm , $\times 10$ magnification). (b) Enlargement of image in (a) shows cellular expression of GFP transgene. Transgene expression occurs in tumor cells (arrows) and possibly in endothelial cells. (c–d) At 6 days after implantation, the tumor vasculature is permeable to EB dye (arrow). Scar vessels, observed on day 6 in vehicle-injected brains, are impermeable to the dye (arrow) despite their abnormal appearance (insets: red, collagen IV; blue, DAPI nuclear stain). Insets in c and d demonstrate collagen-IV antibody-stained vessels associated with tumors (c) or scar (d).

plasmid without BBB disruption targets both solid tumors as well as the STF.

BTB permeability is increased compared to normal BBB

In order to characterize alterations in vascular permeability of tumor-associated vasculature, the distribution of Evans Blue (EB) dye (960.8 MW) after intra-cardiac injection was evaluated in rat brains with and without tumors. Adequate perfusion with the dye was confirmed by demonstrating extravasation of EB in the pineal gland and median eminence, regions known to lack a BBB (not shown). Tumor-associated vessels, but not normal brain vessels, leaked EB at 6, 13 and 17 days after tumor implantation (Figure 2c, arrow).

The trauma and subsequent tissue repair associated with intracerebral injection can promote growth of new vessels (Figure 2d, inset). While EB leakage was prominent in tumor-injected rats at 3 and 6 days after injection (Figure 2c), EB extravasation did not occur in vehicle-injected rats (Figure 2d, arrow). This result demonstrates that only angiogenesis associated with wound healing leads to regeneration of a normal BBB; tumor-associated angiogenesis results in EB leakage.

Therapeutic gene delivery reduces tumor volume and enhances survival

We assessed the therapeutic utility of direct intra-arterial delivery by using a plasmid encoding endostatin (mEndo) to target tumor angiogenesis. Intra-arterial injection of a single dose of 40 μg mEndo plasmid reduced tumor volume by 80% at 13 days, and by 60% at 19 days ($P < 0.05$) when compared to controls. Control

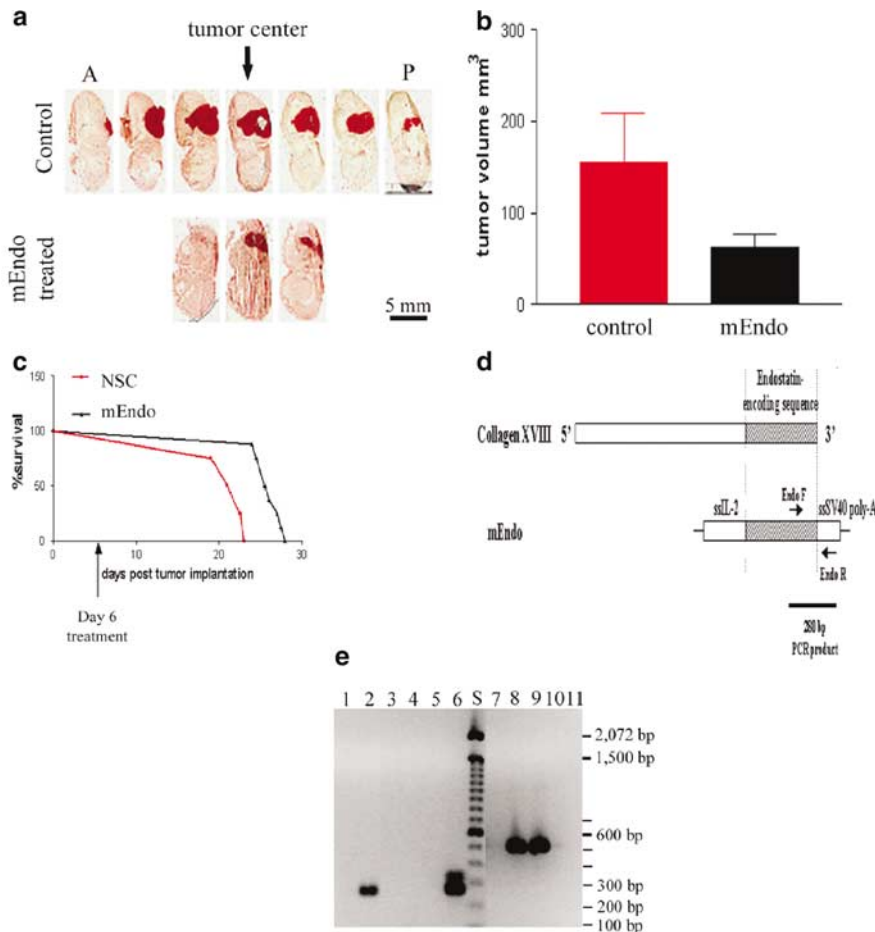


Figure 3 Intra-arterial injection of naked plasmid encoding endostatin decreases tumor volume and increases survival. (a) At 7 days after treatment with endostatin plasmid, 20 μ m thick serial sections of whole brains were obtained and stained in neutral red. Every 10th section is shown with tumor staining dark red. Endostatin-treated animals demonstrate a tumor volume reduction of 80% as compared to control animals ($n=4$ for control, $n=8$ for mEndo). (b) Calculation of tumor volume reduction. BioRad MultiAnalyst software was used to determine tumor area on individual sections and tumor volume was subsequently calculated. (c) Endostatin-treated rats survive 18% longer than untreated rats ($P<0.0002$). (d) Primers were designed to detect plasmid-derived mEndo cDNA but not endogenous collagen XVIII. In order to avoid crossreaction with endogenous endostatin (3' end of collagen XVIII), RT-PCR primers were designed to span the region of plasmid encoding endostatin as well as the linker sequence 5' to the SV40 polyadenylation signal (ssSV40 poly-A). The reverse primer's location within this unique plasmid sequence ensures specific amplification of plasmid-derived endostatin cDNA. (e) RT-PCR analysis demonstrates expression of endostatin in treated but not in control tumors. Primers specific for plasmid-derived endostatin cDNA (endo) showed presence of transcript in mEndo-treated tumor tissue (lane 2) but not in control tumor tissue (lane 4). To ensure that positive signal was not due to plasmid contamination of the mEndo-treated mRNA, preps were PCR-amplified with endo primers prior to reverse transcription. Both treated (lane 1) and untreated (lane 3) tumors did not show plasmid contamination. Controls without template (lane 5) were negative, and plasmid controls (lane 6) showed strong bands. Primers directed against rat α -actin showed equicoalent amounts of mRNA in both mEndo-treated (lane 13) and control (lane 14) tumors. mEndo-treated tumors prior to reverse transcription did not show any contamination with endogenous DNA (lane 12), and controls without template (lane 15) were negative.

animals were either rats implanted with tumor but not treated in any way ('nonsurgical,' data not shown), or rats implanted with tumor and injected intra-arterially with control plasmid (MCS, identical plasmid backbone to mEndo but containing multiple cloning site only) (Figure 3a).

We evaluated the effects of intra-arterial injection of mEndo plasmid on survival in four separate studies. A single intra-arterial injection of mEndo plasmid extended survival by 18% ($P<0.0002$) (Figure 3b). These results were reproduced in four separate survival studies using a total of 26 controls [both nonsurgical ($n=19$) and MCS rats ($n=10$)] and 29 mEndo-treated rats. There was no significant difference in length of survival between MCS (25.5 ± 1.5 days) and NSC rats (27.0 ± 1.5 days). The duration of the effect may be limited by the number of cells transduced with the plasmid as well as the length

of time the plasmid is transcribed and translated. Therefore, the effect on tumor volume becomes less significant as the tumor grows. To prolong the therapeutic effect of endostatin, a fifth survival study was completed using the mEndo/pCEP4 plasmid. This plasmid remains in an episomal state and allows prolonged expression of the endostatin gene. The median survival was extended by 37% ($P<0.03$) and the maximal survival by 47% (data not shown). To illustrate the broader applicability of this delivery method, we also used it to successfully reduce tumor volume with a plasmid encoding herpes simplex virus thymidine kinase (data not shown). In this study, intra-arterial delivery of the thymidine kinase-encoding plasmid followed by ganciclovir administration resulted in a 45% reduction in tumor volume compared with controls (although there were wide variations in the animals tested).

Intra-arterially delivered endostatin is expressed in, and secreted from, tumor cells

Both mEndo and mEndo/pCEP4 plasmids were used to transfect COS and 9L cells in culture. Supernatants from these transfected cells were collected on days 1 and 4 after transfection and tested for endostatin expression by ELISA. At 1 day after transfection, endostatin was not detected in either cell line with either plasmid. By day 4, 9L cells exhibited low levels of expression. COS cells transfected with mEndo plasmid secreted 31.25 ng/ml of supernatant and those transfected with mEndo/pCEP4 secreted 125 ng/ml. The low levels of endostatin expression in 9L cells may be due to the poor transfection efficiency of this cell line in tissue culture.

To determine whether endostatin's effects on tumors and survival were due to systemic expression of transduced plasmid, serum levels of endostatin were measured by ELISA 2 days after intra-arterial delivery of DNA. Endostatin levels did not differ significantly between control (11.5 ± 2.69 ng/ml) and mEndo-treated (15.5 ± 0.84 ng/ml) rats ($P = 0.22$). In addition, intra-arterial injection of a plasmid encoding GFP into tumor-bearing rats demonstrates that GFP-transduced cells are almost exclusively located within the brain tumor; kidney, liver, heart, lungs, spleen and testes did not exhibit GFP expression.

Immunohistochemical analysis of tumors from mEndo-treated rats demonstrated an increase in extracellular endostatin compared to controls (data not shown). However, the epitopes detected by all available anti-endostatin antibodies are present on both endostatin and collagen XVIII. Since tumors express collagen XVIII, primarily on associated vessels,^{13,14} immunohistochemistry is not useful to clearly distinguish endostatin and collagen XVIII levels in tumors. Therefore, we used RT-PCR to detect the presence of plasmid-derived message for mouse endostatin within the tumor tissue. DNase-treated mRNA was reverse transcribed with pd(N)₆ (random hexamer) primers and probed with a primer pair directed against the 3' end of endostatin. In order to avoid crossreaction with endogenous collagen XVIII cDNA, we designed the primers to span the region of the plasmid encoding mouse endostatin and the SV40 polyadenylation signal sequence (Figure 3d). Plasmid-derived endostatin cDNA was detected in tumors 1 day and 2 days after treatment ($n = 3$), but not in NSC tumors ($n = 3$) (Figure 3e).

Endostatin reduces tumor vascular density, perfusion and vascular permeability

In order to characterize the effect of endostatin on the vasculature of treated tumors, we infused fluorescein-dextran (2×10^6 MW) into tail veins of mEndo-treated and control rats. Tumors were immunostained for collagen IV (a marker of vascular basement membrane). Collagen IV-positive vessels were counted to assess tumor vascular density. We confirmed a 59% decrease in average vascular density in mEndo-treated rats compared to MCS rats (Figure 4a) as previously reported.^{7,15} When actual vessel density was calculated, the number for mEndo-treated rats was 187 ± 14 vessels/mm², and 307 ± 30 vessels/mm² ($P < 0.0004$) for the control-treated animals.

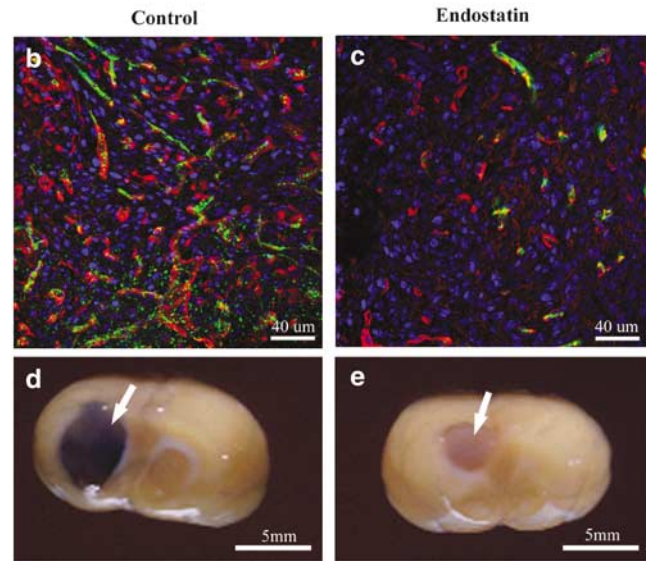
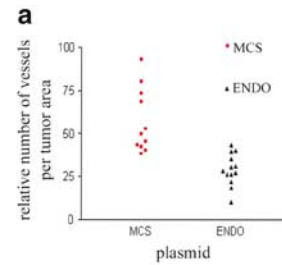


Figure 4 Expression of endostatin decreases tumor vascularity and BTB permeability. (a) The vessel density in endostatin-treated tumors is dramatically decreased by 59% to 187 ± 14 vessels per low-power ($\times 25$) microscopic field (control tumors: 307 ± 30 ($P < 0.0004$)). (b, c) Control tumors (b) are typically highly vascular as shown by the collagen IV stain (red). A higher percentage of vessels appear patent as demonstrated by intracardiac injection of fluorescein-dextran (green) prior to removal of tumor. Endostatin-treated tumors not only show a lower vascular density but also fewer patent vessels (c). (DAPI nuclear stain, blue). (d, e) Rats were injected intracardiac with 4% EB dye. Coronal sections taken through the center of the tumor illustrate the high permeability of the vasculature and resultant extravasation of EB into the tumor parenchyma in control tumors (d, arrow), whereas endostatin-treated tumors (e, arrow) are less permeable to EB.

Untreated tumors showed characteristically hypertrophic and tortuous angiogenic vessels distributed uniformly and at high density throughout the tumor. Vessels were clearly perfused with fluorescein-dextran and in some areas possible leakage of dye into the tumor was observed (Figure 4b). In contrast, mEndo-treated tumors not only demonstrated overall decreased vascular density but also contained completely avascular areas, and perfusion of existing vasculature was decreased or absent (Figure 4c). In addition, the appearance of the treated vasculature more closely resembled that of normal brain rather than tumor vessels.

To determine the effect of endostatin treatment on the physiology of tumor vasculature, mEndo-treated and MCS rats were tested for tumor vessel permeability by EB injection on day 7 after treatment. Tumors in mEndo rats ($n = 6$) showed dramatically reduced permeability to EB dye (Figure 4e, arrow) as compared to tumors in either of the MCS ($n = 6$) or NS ($n = 5$) control groups (Figure 4d, arrow).

Endostatin induces ultrastructural changes in vasculature

NSC, MCS and mEndo-treated brains were examined by transmission electron microscopy for ultrastructural changes in tumor vessel morphology. Blood vessels within both NSC and MCS control tumors were patent (Figure 5a, arrow) and perfused (confirmed by the presence of blood cells, not shown). In contrast, a large percentage of vessel lumens within mEndo-treated tumors (up to 63.7%) were either collapsed (Figure 5b, arrow) or substantially narrowed. No blood cells were observed within these narrowed vessels. In addition, tumor vessels in mEndo-treated rats were surrounded by an increased number of pericytes compared with tumor vessels from NSC or MCS rats. Although considerable variability existed among mEndo animals in the percentage of occluded vessels, no collapsed blood vessels were ever observed in untreated tumors. Remarkably, collapsed vessels were limited to mEndo-treated tumor parenchyma while vessels in surrounding normal brain were unaffected in both control (Figure 5c) and mEndo-treated animals (Figure 5d).

Discussion

The inevitable recurrence of GBM is thought to result from satellite tumor foci (STF) that result from migration of tumor cell(s) a short distance from the main tumor mass, escape surgical resection and resist radiation and chemotherapy. The BTB, although more permeable than

BBB, is still highly impermeable to most chemotherapeutic agents¹⁶ and viral vectors without BTB disruption.^{10,17} In this study, we show that the permeability of the BTB itself is sufficient to permit the specific and efficient delivery of plasmid DNA to brain tumors and STF. Targeting to STF, as well as the main tumor mass, provides a significant advantage over current gene therapeutic strategies that do not effectively target STF. Direct and selective transduction of tumor cells by plasmids encoding therapeutic genes is an appealing strategy since it provides a high local level of the gene product, reducing potentially harmful systemic effects. In addition, the use of 'naked' plasmids has not been shown to elicit a strong immune response, particularly in comparison to the immune response observed with most viral vectors routinely used to deliver transgenes.¹⁸

GBM's highly vascular nature suggests that it may be a good target disease for antiangiogenic therapy. We show that intra-arterial delivery of a plasmid encoding endostatin leads to decreased tumor volume, decreased vascular density and increased survival in the rat 9L gliosarcoma model. This model closely resembles GBM in humans, but it is even more lethal and aggressive; the median survival is only 25 days following implantation. Similar results using angiostatic agents to treat GBM have been reported in a subcutaneous tumor model as well as in an orthotopic model using encapsulated endostatin-secreting cells, which were implanted simultaneously with tumor cells.⁹ Our data differ from these earlier reports in that we demonstrate therapeutic efficacy of endostatin plasmid administered to an already established tumor. This is more relevant to the situation seen clinically in humans; most patients presenting with GBM already have established tumor. In addition, we demonstrate endostatin's dramatic effect on vascular physiology and ultrastructure. Vascular permeability is reduced and vessels within mEndo-treated tumors are collapsed. This narrowing of the blood vessel lumens may decrease blood flow to the tumor, reducing supply of oxygen and nutrients essential for continued growth. Endostatin's effect on vessel lumen patency has been previously reported in a wound-healing model¹⁹ but not in tumors. While the improvement in survival is modest, it is statistically significant in this highly reproducible and aggressive model.

The phenomenon of tumor cells homing toward blood vessels has been described.^{20,21} A similar finding has been observed with malignant gliomas in humans.²² The close association between tumor and blood vessels suggests that an intra-arterial approach may be effective in targeting satellite lesions as well as primary tumors. After a single intra-arterial injection of mEndo plasmid, we observed decreased tumor load but not total eradication of the tumor. This may be due to variability in transduction efficiency of cells within the tumor or limited transgene expression; if the cells effectively transduced by the plasmid ultimately die due to the therapeutic effect of the endostatin, long-term efficacy of the treatment would be compromised, leaving a survivor tumor cell population that could regrow. Combination gene therapy, sequential drug treatment or other small molecule therapeutics may prove more effective combined with an antiangiogenic agent that slows tumor progression and widens the therapeutic window. This

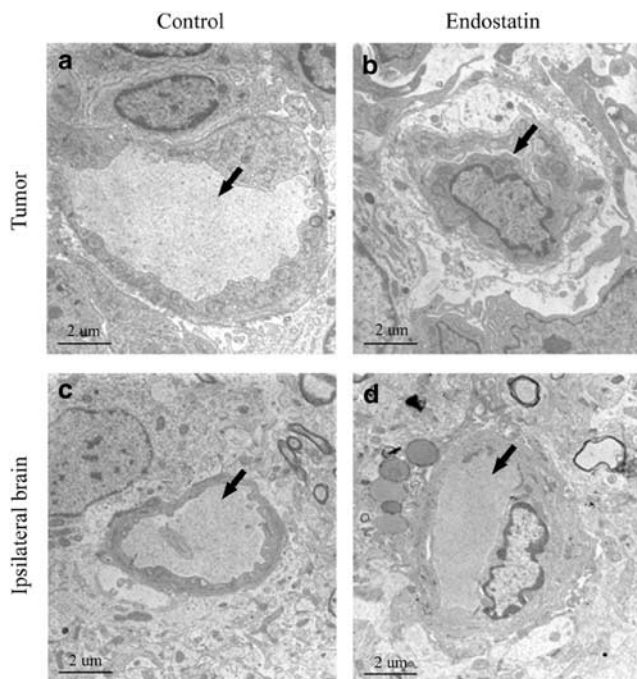


Figure 5 Endostatin alters vascular perfusion by altering vascular ultrastructure. (a) Blood vessels within control tumors display open lumens (arrowhead) allowing blood flow. (b) Up to 63% of vessels within endostatin-treated tumors have collapsed lumens (arrowhead), which may obstruct blood flow. (c, d) In contrast, normal brain around tumor in both control (c) and mEndo-treated (d) animals show patent and perfused vessels. Magnification: $\times 6610$.

strategy may be even more efficacious in human tumors that generally cycle more slowly than rodent tumor models²³ and thus, provide a broader therapeutic window within which to treat. Our observations with intra-arterial delivery of a plasmid encoding a suicide gene (HSV-TK in combination with gancyclovir, data not shown) also reduced tumor volume, suggesting that this, combined with an antiangiogenic, may be a more efficacious therapy. Such combination therapy, delivered intra-arterially using 'naked' plasmids, should have broad applicability to the treatment of tumors and, more specifically, may be useful in the treatment of both primary and metastatic brain tumors.

Materials and methods

Plasmid vectors

pEGFP-N1 plasmid was purchased from Clontech (Palo Alto, CA, USA). The plasmids pblast-mEndo, pblast-mcs, pGT59 (HSV-Tk) were purchased from InvivoGen (San Diego, CA, USA). Plasmids were purified and tested for endotoxin contamination (<0.1 EU/ μ g plasmid). The plasmid pCEP4 (Invitrogen, Carlsbad, CA, USA) was used to construct mEndo/pCEP4 by ligating the mEndo fragment from pblast-mEndo into the multiple cloning site of pCEP4.

Tumor implantation and intra-arterial delivery

Solitary intracerebral 9L tumors were established in adult male CD Fischer 344 rats weighing 250–300 g (Charles River Laboratories, Wilmington, MA, USA) by stereotactic implantation of 5×10^4 9L gliosarcoma cells (gift from Xandra Breakefield) in 2 μ l of OptiMEM (GibcoBRL Life Technologies, Rockville, MD, USA) into the right frontal lobe. Implantation technique and anesthesia were performed as previously described.¹⁷ Sham surgeries, identical to tumor implantation procedures with the exception of the tumor cell injection, were performed on control animals. At 6 days after tumor implantation, rats were anesthetized. Through a midline anterior neck incision, the common carotid artery was isolated. The external carotid artery was tied off above the bifurcation with a 4-0 silk suture. Using a 30-gauge needle attached to polyethylene PE-10 tubing (Intramedic Clay-Adams brand, Becton Dickinson, Sparks, MD, USA), the common carotid was accessed and plasmid DNA or vehicle (Opti MEM, GibcoBRL Life Technologies, Rockville, MD, USA) in a 200 μ l volume was infused followed by 800 μ l flush with vehicle over 1 min. The needle was withdrawn and the hole sealed with Vetbond (3 M Animal Care Products, St Paul, MN, USA).

All animal procedures were performed in compliance with institutional animal care guidelines. Control and experimental rats in thymidine kinase experiment were treated with 30 mg/kg gancyclovir (GCV) (InvivoGen, San Diego, CA, USA) i.p. twice daily.

EB experiments

Tumor- or control (sham surgeries) rats were given an anesthetic overdose using ketamine and xylazine (0.6 ml of 50:50 solution). EB (4% in $1 \times$ PBS, w/v, Sigma, St Louis, MO, USA) was injected into the left ventricle of the heart and allowed to circulate for 90 s. Residual

intravascular EB was flushed out with $1 \times$ PBS, the brain removed, sectioned and photographed.

Light microscopy and immunohistochemistry

Rats were anesthetized with a lethal dose of ketamine and xylazine and perfused with PBS followed by Prefer fixative (Anatech Ltd, Battle Creek, MI, USA). Brains were postfixed in Prefer for 4 h and then saturated in 20% sucrose in PBS overnight. Tissues were mounted in O.C.T. compound (Miles, Elkhart, IN, USA), frozen at -80°C , and sectioned on a Leica cryostat.

For immunohistochemistry, 20 μ m thick sections were incubated with either rabbit-anti-mouse collagen IV diluted 1:200 from Chemicon (Temecula, CA, USA) or rabbit-anti-mouse endostatin diluted 1:200 from Chemicon (Temecula, CA, USA) followed by the appropriate secondary antibody conjugated to Alexa dyes (Alexa 594-conjugated goat-anti-rabbit IgG 1:200, Molecular Probes, Eugene, OR, USA). Sections were then mounted in DAPI-containing mounting medium (Vectashield, Vector Laboratories, Burlingame, CA, USA) and imaged on a Biorad 1024 multiphoton system (Hercules, CA, USA).

Tumor volume analysis was performed by serial sectioning entire tumors, staining with neutral red and measuring tumor area per section scanned into computer using the BioRad model GS-700 imaging densitometer. Tumor area and volume were determined using Multi-Analyst software (BioRad, Hercules, CA, USA).

RT-PCR

Animals were anesthetized and perfused with $1 \times$ PBS followed by RNA later (Ambion, Austin, TX, USA). Brains were removed and stored in RNAlater at -20°C . mRNA was isolated using the Micro-FastTrack 2.0 Kit (Invitrogen, Carlsbad, CA, USA). To eliminate any contaminating genomic or plasmid DNA, mRNA was DNase treated using DNA-free (Ambion, Austin, TX, USA), and then reverse transcribed using the First Strand cDNA synthesis kit (Amersham Pharmacia, Piscataway, NJ, USA). PCR was performed using Taq DNA polymerase (Amersham Pharmacia, Piscataway, NJ, USA) using 5'-AGAAGAGCGTATGGCAGC-3' as forward primer and 5'-CAAATCATCAATGTATCTTATCATGTC-3' as reverse to detect plasmid-derived endostatin and 5'-ACCCAGATCATGTTTGAGACC-3' and 5'-AGCACTGTGTTGGCATAGAGG-3' to detect rat α -actin. All primers were purchased from Genset Oligos (La Jolla, CA, USA). Reactions were amplified on a Perkin-Elmer PCR cyler and imaged on a Biorad Chemidoc fluorescent imager.

Electron microscopy

Unperfused tumor tissue was immersion fixed in 4% paraformaldehyde, 1.5% glutaraldehyde in 0.1 M cacodylate buffer pH 7.3 (Electron Microscopy Sciences, Fort Washington, PA, USA). After fixation, the tumors were minced and postfixed. Samples were washed in 0.1 M cacodylate buffer, fixed in 1% osmium tetroxide, dehydrated through ethanol, cleared in propylene oxide, and rotated in a mix of propylene oxide and Epon/Araldite. Samples were placed in 100% resin and mounted in embedding molds and polymerized at 60° for 24 h. Ultrathin sections were cut using a diamond knife (Reichert Ultracut E, Diatome, Fort Washington, PA, USA), placed on parlodion-coated copper slot grids, and

stained with uranyl acetate and lead citrate. Grids were examined on a Philips CM-100 electron microscope. Images were documented using Kodak SO-163 film. To quantify occluded vessels, nonconsecutive thin sections within each tumor as well as normal brain were examined and classified independently by three observers. Occluded, vessel lumens measured <0.5 μm in diameter. The size of narrowed vessels ranged from 0.5 to 1 μm .

ELISA

Supernatants of cultured COS and 9L cells transfected with endostatin plasmid as well as rat sera were tested for endostatin expression. Quantitation was performed using ChemiKine mouse endostatin EIA kit (Chemicon, Temecula, CA, USA) according to the manufacturer's instructions.

Transfections

COS and 9L cells were cultured in DMEM (GibcoBRL Life Technologies, Rockville, MD, USA), supplemented with 10% fetal calf serum. Transfections were carried out using Lipofectamine (Invitrogen, Carlsbad, CA, USA) according to the manufacturer's instructions.

Acknowledgements

This work was supported by grants to MF from the National Eye Institute R24EY14174 and the Robert Mealey Program for the Study of Macular Degenerations. FB is a Skaggs Scholar in Clinical Science and receives grant support from the Skaggs Program. We are grateful to numerous members of the Friedlander Laboratory for assistance in various aspects of this project and to the staff and veterinarians of the LARC at TSRI for their excellent assistance.

References

- Kramm CM *et al*. Gene therapy for brain tumors. *Brain Pathol* 1995; **5**: 345–381.
- Lam PY, Breakefield XO. Potential of gene therapy for brain tumors. *Hum Mol Genet* 2001; **10**: 777–787.
- Boehm T, Folkman J, Browder T, O'Reilly MS. Antiangiogenic therapy of experimental cancer does not induce acquired drug resistance. *Nature* 1997; **390**: 404–407.
- Folkman J. Angiogenesis in cancer, vascular, rheumatoid and other disease. *Nat Med* 1995; **1**: 27–31.
- Carmeliet P, Jain RK. Angiogenesis in cancer and other diseases. *Nature* 2000; **407**: 249–257.
- O'Reilly MS *et al*. Endostatin: an endogenous inhibitor of angiogenesis and tumor growth. *Cell* 1997; **88**: 277–285.
- Blezniger P *et al*. Systemic inhibition of tumor growth and tumor metastases by intramuscular administration of the endostatin gene. *Nat Biotechnol* 1999; **17**: 343–348.
- Chen QR, Kumar D, Stass SA, Mixson AJ. Liposomes complexed to plasmids encoding angiostatin and endostatin inhibit breast cancer in nude mice. *Cancer Research* 1999; **59**: 3308–3312.
- Read TA *et al*. Local endostatin treatment of gliomas administered by microencapsulated producer cells. *Nat Biotechnol* 2001; **19**: 29–34.
- Barnett FH *et al*. Selective delivery of herpes virus vectors to experimental brain tumors using RMP-7. *Cancer Gene Ther* 1999; **6**: 14–20.
- Rainov NG *et al*. Intra-arterial virus and nonvirus vector-mediated gene transfer to experimental rat brain tumors. *Front Radiat Ther Oncol* 1999; **33**: 227–240.
- Rainov NG *et al*. Intraarterial delivery of adenovirus vectors and liposome–DNA complexes to experimental brain neoplasms. *Hum Gene Ther* 1999; **10**: 311–318.
- Kuo CJ *et al*. Oligomerization-dependent regulation of motility and morphogenesis by the collagen XVIII NC1/endostatin domain. *J Cell Biol* 2001; **152**: 1233–1246.
- Musso O *et al*. Tumor hepatocytes and basement membrane-producing cells specifically express two different forms of the endostatin precursor, collagen XVIII, in human liver cancers. *Hepatology* 2001; **33**: 868–876.
- Sauter BV *et al*. Adenovirus-mediated gene transfer of endostatin *in vivo* results in high level of transgene expression and inhibition of tumor growth and metastases. *Proc Natl Acad Sci USA* 2000; **97**: 4802–4807.
- Kroll RA *et al*. Improving drug delivery to intracerebral tumor and surrounding brain in a rodent model: a comparison of osmotic *versus* bradykinin modification of the blood–brain and/or blood–tumor barriers. *Neurosurgery* 1998; **43**: 879–886; discussion 886–879.
- Rainov NG *et al*. Selective uptake of viral and monocrySTALLINE particles delivered intra-arterially to experimental brain neoplasms. *Hum Gene Ther* 1995; **6**: 1543–1552.
- Loser P *et al*. Advances in the development of non-human viral DNA-vectors for gene delivery. *Curr Gene Ther* 2002; **2**: 161–171.
- Bloch W *et al*. The angiogenesis inhibitor endostatin impairs blood vessel maturation during wound healing. *FASEB J* 2000; **14**: 2373–2376.
- Zagzag D *et al*. Vascular apoptosis and involution in gliomas precede neovascularization: a novel concept for glioma growth and angiogenesis. *Labor Invest* 2000; **80**: 837–849.
- Holash J, Wiegand SJ, Yancopoulos GD. New model of tumor angiogenesis: dynamic balance between vessel regression and growth mediated by angiopoietins and VEGF. *Oncogene* 1999; **18**: 5356–5362.
- Chan PT, Weller RO. Factors influencing tumour cell and vascular proliferation in glioblastoma. *Neuropathol Appl Neurobiol* 2002; **28**: 155–156.
- Ram Z *et al*. Therapy of malignant brain tumors by intratumoral implantation of retroviral vector-producing cells. *Nat Med* 1997; **3**: 1354–1361.